SIXTH EUROPEAN ROTORCRAFT AND POWERED LIFT AIRCRAFT FORUM

Paper No. 44

LATERAL FLUTTER OF LOADS TOWED BENEATH HELICOPTERS AND ITS AVOIDANCE

A. Simpson and J. W. Flower

University of Bristol, England.

Septermber 16-19, 1980

Bristol, England.

THE UNIVERSITY, BRISTOL, BS8 1HR, ENGLAND.

LATERAL FLUTTER OF LOADS TOWED BENEATH HELICOPTERS AND ITS AVOIDANCE

A. Simpson and J. W. Flower

University of Bristol, England.

ABSTRACT

In this paper, we address the problem of aerodynamic instability of strop-supported freight loads. Part I of the paper concerns an in-depth study of the lateral, low frequency flutter of rectangular cargo containers supported by multi-strop arrangements. For certain strop arrangements, it is shown that necessary conditions for flutter and divergence may be obtained in which the primary parameters are the static strop tensions at the current forward speed. These criteria enable rapid assessment of lateral stability when only the longitudinal static aerodynamic characteristics are available. Part II of the paper comprises an overview of the state of the art of aerodynamics (steady and unsteady) of towed shapes, and highlights the need for more fundamental research in this area.

1. INTRODUCTION

The problems of instability of helicopter underslung loads reached their zenith in the Vietnam War where, due principally to the efficiency of the external mode of freight and troop conveyance as reflected in short turn-around times, this mode of transport was being extensively used. Several major contracts were placed by the U.S.Army during this period concerning the aerodynamics, stability and stabilisation of underslung loads - the contract work being typified by the reports of References 1, 2 and 3 and by the AGARD paper[4], based on the work of Reference 3. At the end of the Vietnam War, interest flagged to the extent that no further U.S. contracts were placed. Individual U.K. work (typified by References 5 and 6) regrettably followed suit, and at the present time, no substantial research effort is being exerted in this area - at least, not to the knowledge of the authors. Furthermore, very recent representations made to the authors from within the U.K. suggested that much of what had been accomplished during the early 1970's had been forgotten! Since dynamic instability is the major envelope-limiting feature of this vital mode of freightage, it is important that the initiative taken by the U.S. Army in motivating research in this area at the beginning of the last decade is not completely lost, for if it were, any future applications would involve reversion to the expensive ad hoc stability-clearance exercises so common in the 1960's. The major objective of this paper is to re-vitalise interest by completing ä simple, passive load stabilisation study started in 1975 and by pointing to areas where research of a fundamental nature is required.

In References 1-6, much emphasis is placed on the study of the aerodynamics and stability of underslung rectangular cargo containers, typified by the standard 20' x 8' x 8' and 40' x 8' x 8' shapes, and rather less so by the 8' x 8' x 8' shape, in view of the emergence of the 'containerisation' philosophy. Some earlier work[7] had dealt with underslung pallets, this being the first study in which the importance of frequency parameter on the aerodynamic forces had been recognised. This unsteady aspect of the aerodynamic forces, extended by considerations of the effects of free stream turbulence, was emphasised in References 3 and 4 in relation to the 5:2:2 container shape and was shown to have an important bearing on dynamic stability in certain 'high-frequency' modes of such a container, typically stropped. However, in many cases, the envelope-limiting feature is not 'high frequency' oscillation of the suspended load, but rather 'low-frequency' pendulous oscillation of large amplitude associated with relatively high forward speed of the helicopter - this implying low frequency parameter and the concomitant possibility of the use of quasi-steady aerodynamics when attempting to predict instability or to design stabilisation systems. Incipiently, such low frequency instability modes are predominantly lateral, involving sideslip and yaw as their principal components, but if allowed to develop these will couple, strongly in some cases, with longitudinal motion and may involve amplitudes so large that it is necessary to jettison the container.

In the first part of this paper we shall address the problem of low frequency oscillation of 5:2:2 and 5:1:1 container shapes restrained by a very rudimentary form of stropping. We shall see that some very simple guidelines for stabilisation may be deduced from the fact that the basic instability mode is merely an instance of classical flutter in sideslip

and yaw. These guidelines are thought to be new, aside from their appearance in a simplified form in Reference 3, and to offer potential for passive stabilisation of rectangular container loads, as against active stabilisation[2] which is costly. Even if some form of active stabilisation proves to be necessary, a knowledge of passive stabilisation laws is invaluable in limiting the sizes of auxiliary jacks, hydraulic supplies, etc., or the amount of feedback to the helicopter ASE required to ensure complete vehicle/load stability - bearing in mind that the ASE is designed with the helicopter per se in view and that any overt additional demands on it may prove unacceptable unless its capacity is increased.

In the second part of the paper, we shall address the more general problem of what further unsteady aerodynamics work might be required for a coherent (as distinct from ad hoc) philosophy of underslung load stabilisation, including 'high frequency' oscillation effects. The U.S.-sponsored work of the early 1970's had merely scratched the surface of this subject, Reference 3 representing the only research in this area known to the authors.

2. PART I THE LATERAL FLUTTER OF UNDERSLUNG RECTANGULAR CONTAINER LOADS

2.1 AVOIDANCE OF SINGLE DEGREE-OF-FREEDOM FLUTTER PHENOMENA

If single strop arrangements are employed to suspend 5:2:2 or 5:1:1 containers (Figure 1a), the containers will invariably rotate to adopt the major-axis crosswind (maximum drag) orientation as soon as the helicopter moves forward in still air. This is clearly undesirable from the viewpoint of freightage efficiency, and the undesirability is accentuated by the fact that yaw oscillations will inevitably occur in a limit cycle whose amplitude is governed totally by forward speed. For while the container is statically stable in its maximum drag configuration, Refs 3 and 4 show that it is dynamically unstable (orbitally stable). These stability phenomena have also been discussed and mathematically modelled in Reference 8, which, however, does not allow for the effects of frequency parameter.

In order to avoid conveyance in the maximum drag configuration, yaw restraint is required, and this may be most simply provided by recourse to a twin strop support configuration (Figure 1b). If the yaw restraint provided by the strops is adequate, the 5:2:2 and 5:1:1 containers will be conveyed in their minimum drag (major axis windward) positions, although with inclined strops there will be some steady departures in pitch, growing with speed. Now References 1 and 3 show that the 5:2:2 and 5:1:1 containers are statically stable in pitch and yaw for departure angles from the minimum drag position of about 10° and 3° respectively with respect to central minor axes, while References 3 and 4 show both containers to be strongly dynamically unstable in pitch and yaw about these same axes. The dynamical instability in pitch is of no consequence when twin strops are employed, since pitch is intrinsically coupled to fore-and-aft (and perhaps heave) motions which are strongly dumped. However, the dynamical instability in yaw is largely unconstrained and will therefore persist, perhaps coupling with sideslip and the longitudinal motions.

The obnoxious single degree-of-freedom yaw flutter may be avoided by nosing the containers up or down (12°-15° for the 5:2:2 container and 5°-10° for the 5:1:1 container) at the expense of additional drag. The basis for this is to be found in Reference 3 where dynamic stability loop diagrams are presented. However, nosing up will produce positive lift which will ultimately lead to strop slackening and loss of restraint. Hence, nosing down provides the only practical solution, but at the expense of increasing apparent weight with increasing forward speed as well as increased drag.

Having dispensed with the single-degree-of-freedom flutter modes, we now have to address the major remaining problem, viz, classical lateral flutter, involving yaw and sideslip as its dominant constituents.

2.2 CLASSICAL LATERAL FLUTTER: QUASI-STEADY THEORY

We consider a rectangular container supported by four symmetrically disposed, parallel, inextensible strops of length $\bar{\ell}$, in a nose-down attitude, Θ, as shown in Figure 2. Consideration of strop-container kinematics, assuming the container to be perfectly rigid, shows that sideslip, $\bar{y}$, is uncoupled from yaw, ψ, and roll, ϕ, but that

$$\phi = -T\psi \qquad \ldots\ldots\ldots\ldots\ldots\ldots\ldots\ldots \quad (1)$$

for small departures ϕ and ψ, where $T = \tan(\theta-\Theta)$; θ being the swing-back angle of the strops at speed V. There is no change of container attitude with V because the strops are parallel and of equal length. We shall assume that

(i) The helicopter flies straight and level in still air, or a direct headwind, and that there are no dynamic departures of the aircraft from this simple equilibrium state - whether natural or pilot induced.

(ii) Container motion is of sufficiently low frequency that quasi-steady aerodynamic assumptions are valid, and is of small amplitude to allow the use of linear dynamical theory.

(iii) The container CG lies in the vertical plane of symmetry of the container.

(iv) Nose-down incidence, Θ, is such that container yaw motion *per se* is dynamically stable.

(v) Rotor downwash effects on the container are negligible.

(vi) Aerodynamic moments acting on the container are referred to axes which pass through its geometric centre, C.

A convenient dimensionless measure of container forward velocity, V, is the Froude number, F, defined by

$$V^2 = g\bar{d}F^2 \qquad \ldots\ldots\ldots\ldots\ldots\ldots\ldots\ldots \quad (2)$$

All lengths shown in Figure 2 will be rendered dimensioness by division by container length, $\bar{d}$. Aerodynamic force and moment coefficients will be based on $\bar{h}^2$ and $\bar{h}^2\bar{d}$ respectively, while the respective angular rate derivatives will be based on $\bar{h}^2\bar{d}$ and $\bar{h}^2\bar{d}^2$. The basic equilibrium variables will be the dimensionless strop tensions, $T_1 = \bar{T}_1/mg$ and $T_2 = \bar{T}_2/mg$ where in view of assumptions (i) and (iii), the forward strops each carry tension $\bar{T}_1/2$ and the leeward ones $\bar{T}_2/2$. Additionally, it will

be assumed that aerodynamic actions on the strops themselves are negligible. An additional equilibrium variable is, of course, θ.

The equations of equilibrium in dimensionless form may be obtained by inspection of Figure 2. They are:-

$$\tan\theta = \mu F^2 C_D/(\mu F^2 C_L + 1)$$

$$T_1+T_2 = \sec\theta\,(\mu F^2 C_L + 1) \qquad (3)$$

$$\text{and} \quad r \equiv \frac{T_2}{T_1} = \frac{(a-x)c + \left(\frac{h}{2}+z\right)s + \mu F^2\left\{C_L\left(ac+\frac{h}{2}s\right)-C_D\left(\frac{h}{2}c-as\right)-C_M\right\}}{(b+x)c - \left(\frac{h}{2}+z\right)s + \mu F^2\left\{C_L\left(bc-\frac{h}{2}s\right)+C_D\left(\frac{h}{2}c+bs\right)+C_M\right\}}$$

where $\mu = \rho\bar{h}^2\bar{d}/2m$ = relative density/2 . . . . . (3a)

$s = \sin\Theta$, $c = \cos\Theta$ . . . . . (3b)

A Lagrangian analysis of the linear lateral dynamics of the container, in which $y = \bar{y}/\bar{d}$ and ψ are used as generalised coordinates and $\tau = Vt/\bar{d}$ as dimensionless time, leads to the dimensionless equations of motion

$$(\underset{\sim}{A} + \mu\underset{\sim}{\mathfrak{I}})\,\ddot{\underset{\sim}{q}} + \mu\underset{\sim}{B}\,\dot{\underset{\sim}{q}} + (\chi\underset{\sim}{E} + \mu\underset{\sim}{C})\,\underset{\sim}{q} = \underset{\sim}{0} \qquad (4)$$

wherein $\chi = T_1/\ell F^2$ . . . . . (4a)

$\underset{\sim}{q} = \{y, \psi\}$ . . . . . (4b)

$\underset{\sim}{A} \equiv$ structural mass matrix $= \begin{bmatrix} 1, & R \\ R, & R^2+k_\psi^2+k_\phi^2T^2 \end{bmatrix}$ . . . . . (4c)

$R \equiv$ C.G. position factor $= x + zT$ . . . . . (4d)

k_ψ, k_ϕ = dimensionless yaw, roll radii of gyration about axes through G (4e)

$\underset{\sim}{\mathfrak{I}} \equiv$ virtual inertia matrix $= \pi\,\mathrm{Diag}\left[1, (h+1)^2/16h + h^2/4\right]$ . . . . . (4f)

$\underset{\sim}{B} \equiv$ aerodynamic damping matrix $= \begin{bmatrix} (C_{y\bar{\psi}} + C_D s^2)\sec\Theta, & -C_{y\dot{\psi}} \\ (C_{N\bar{\psi}}\cos\theta - C_{\ell\bar{\psi}}\sin\theta)\sec\Theta\Sigma, & -C_{N\dot{\psi}} \end{bmatrix}$ (4g)

$\underset{\sim}{C} \equiv$ aerodynamic stiffness matrix $= \begin{bmatrix} 0, & -\sec\Theta\{C_{y\bar{\psi}}+(cC_L+sC_D)\Sigma\sin\theta\} \\ 0, & -\Sigma\sec\Theta\,(C_{N\bar{\psi}}\cos\theta - C_{\ell\bar{\psi}}\sin\theta) \end{bmatrix}$ . . (4h)

$E \equiv$ structural stiffness matrix $= \begin{bmatrix} 1+r, & \alpha-\beta r \\ \alpha-\beta r, & \alpha^2+\beta^2 r+\varepsilon^2\Sigma^2(1+r) \end{bmatrix}$ . . . . . (4i)

$\alpha = a - \frac{h}{2}T$, $\beta = b + \frac{h}{2}T$, $\Sigma = \sec(\theta-\Theta)$ . . . . . (4j)

and the dot denotes $d/d\tau$.

In equations (4g) and (4h), the static coefficients and derivatives are such that the wind tunnel test results of Reference 1 may be used directly. In Reference 1, forces D, L, Y are measured on tunnel axes, as are the moments ℓ, M, N, as functions of $\bar{\psi}$ (tunnel axis yaw angle) and $\bar{\Theta}$ (tunnel axis pitch angle), where $\bar{\psi} = \psi\sec\Theta$, $\bar{\Theta} = \Theta$ for the cases to be

studied here. The damping derivative $C_{N\dot{\psi}}$ may be obtained, for 5:2:2 and 5:1:1 container shapes, from Section 6 of Reference 3. Unfortunately, $C_{Y\dot{\psi}}$ is not available for the specific cases to be considered, but the results of Reference 3 show it to be positive and of value between 1 and 2 times $|C_{N\dot{\psi}}|$. In the cases to be studied here, $C_{N\dot{\psi}}$ is positive while the contribution of $C_{\ell\dot{\psi}}$ is small - hence the effect of $C_{Y\dot{\psi}}$ (positive) will always be such as to enhance aerodynamic damping (i.e. $\underset{\sim}{B}$ will be a positive definite matrix).

The derivation of eqn. (4) is straightforward and perfectly standard and is therefore not presented here. The method of solution for flutter and divergence boundaries via Routh's criteria used in the desk-top computer solutions of eqn. (4) is also standard and need not be remarked upon further. Before proceeding to the numerical solutions of eqn. (4), however, we shall draw some important inferences from 'undamped' theory.

2.3 SOME INFERENCES FROM QUASI-STEADY UNDAMPED FLUTTER THEORY

It has been remarked that $\underset{\sim}{B}$ will be pos. def. when angle Θ is assigned appropriately. Under such circumstances, any flutter of the container will be stiffness driven and, for the most part, may be investigated by using undamped flutter theory. Also, in practice, μ will be less than 0.02 (usually) so that $\underset{\sim}{\mu}$ may be disregarded. With $\underset{\sim}{\mu} = \underset{\sim}{B} = \underset{\sim}{0}$, eqn. (4) becomes

$$\ddot{\underset{\sim}{q}} + \overline{\underset{\sim}{\Gamma}}\, \underset{\sim}{q} = \underset{\sim}{0} \qquad \ldots\ldots\ldots\ldots\ldots\ldots\ldots\ldots \quad (5)$$

where $\overline{\underset{\sim}{\Gamma}} = \underset{\sim}{A}^{-1}\left[\chi\, \underset{\sim}{E} + \mu\, \underset{\sim}{C}\right]$. It is convenient to take a change of axes

$$\underset{\sim}{q} \equiv \begin{bmatrix} y \\ \psi \end{bmatrix} = \begin{bmatrix} 1, & -R \\ 0, & 1 \end{bmatrix} \begin{bmatrix} y' \\ \psi \end{bmatrix} \equiv \underset{\sim}{W}\, \underset{\sim}{q}' \qquad \ldots\ldots\ldots\ldots\ldots \quad (6)$$

so that eqn (5) becomes $\ddot{\underset{\sim}{q}}' + \underset{\sim}{\Gamma}\, \underset{\sim}{q}' = \underset{\sim}{0}$ $\qquad \ldots\ldots\ldots\ldots\ldots \quad (7)$

where now $\underset{\sim}{\Gamma} = \underset{\sim}{W}^{-1}\, \overline{\underset{\sim}{\Gamma}}\, \underset{\sim}{W}$. Writing $\underset{\sim}{q}' \equiv \underset{\sim}{q}'e^{\lambda\tau}$ we obtain the condition

$$\left|\lambda^2 \underset{\sim}{I} + \underset{\sim}{\Gamma}\right| \equiv \lambda^4 + \lambda^2(\Gamma_{11}+\Gamma_{22}) + \Gamma_{11}\Gamma_{22} - \Gamma_{12}\Gamma_{21} = 0 \qquad \ldots\ldots \quad (8)$$

for a nontrivial $\underset{\sim}{q}'$ solution of eqn (7). The λ^2 solutions of eqn (8) are given by

$$2\lambda^2 = -(\Gamma_{11}+\Gamma_{22}) \pm \{(\Gamma_{11}-\Gamma_{22})^2 + 4\,\Gamma_{12}\Gamma_{21}\}^{\frac{1}{2}} \qquad \ldots\ldots\ldots \quad (9)$$

and complex values of λ (implying flutter) can occur only if the surd is imaginary, i.e. if Γ_{12} and Γ_{21} are of opposite sign. On use of eqns (4c), (4h), (4i) and (6), a necessary condition for flutter is found to be

$$Q \equiv \Gamma_{12}/\Gamma_{21} = K^2\left[\frac{\alpha - R - r(\beta+R) + \frac{\mu}{\chi}C_{12}}{\alpha - R - r(\beta+R)}\right] < 0 \qquad \ldots\ldots\ldots \quad (10)$$

Now for the 5:2:2 and 5:1:1 containers, and many other shapes (but not the 1:1:1 container), C_{12} is negative (and strongly so for 5:2:2 and 5:1:1 containers stropped as in Figure 2 with Θ small). It follows from condition (10) that a necessary condition for flutter is

$$\frac{\alpha - R - \frac{\mu}{\chi}|C_{12}|}{\beta+R} < r < \frac{\alpha - R}{\beta+R} \qquad \ldots\ldots\ldots\ldots\ldots\ldots \quad (10A$$

The lower limit on r may be disregarded since by choosing V sufficiently large, we may make χ as small as we like. Condition (10A) thus reduces to

$$r \equiv \frac{T_2}{T_1} < \frac{a-x-\left(\frac{h}{2}+z\right)\tan(\theta-\Theta)}{b+x+\left(\frac{h}{2}+z\right)\tan(\theta-\Theta)} \quad \ldots\ldots\ldots\ldots\ldots\ldots \quad (11)$$

Eqn (3) defines r and θ as functions of F, and to avoid flutter we need to maintain r as large as possible, vide criterion (11). From eqn (3) we see that the C_L term assists us through the moment $\frac{h}{2}\,s\,C_L$ (C_L being positive for $\Theta < 90^\circ$ for the 5:2:2 and 5:1:1 shapes), but only in a minor way when Θ is small. The C_D term, however, opposes us through the moments $\frac{h}{2}\,c\,C_D$ and $(b-a)\,s\,C_D$, but only moderately since h/2 = 0.2 (5:2:2), 0.1 (5:1:1) and b-a will usually be small. The C_M term is of the greatest interest since it provides us with some latitude for flutter prevention - particularly for the 5:2:2 shape for which $C_{M_o} < 0$ for $\Theta < 20^\circ$ (see Figure 3), while $C_{N\dot{\psi}}$ is negative above $\Theta \approx 10^\circ$. Negative C_M clearly exerts a beneficial influence on r in relation to criterion (11).

It is significant to note that by conjoining condition (11) and eqns (3), we have a criterion for lateral flutter, or its prevention, based wholly on longitudinal static forces, e.g. C_D, C_L and C_M. This is hardly surprising when we reflect on classical wing flutter theory, because variation of r is equivalent to variation of the position of the flexural axis. If $r > \frac{\alpha-R}{\beta+R}$, the 'flexural axis' is aft of G - a condition which is known to be flutter-free. Conversely, if $r < \frac{\alpha-R}{\beta+R}$, G is aft of the 'flexural axis' - a condition which is known to foment flutter.

Note that the use of undamped theory precludes the possibility of prediction of flutter conditions not associated with frequency coalescence; i.e. damping-stiffness or inertia-damping coupled flutter phenomena. If, however, $C_{N\dot{\psi}}$ is sufficiently negative, such phenomena will not occur - and this again means a suitable choice of Θ. It should also be noted that the accuracy of full flutter predictions afforded by undamped theory will be greater for smaller than for larger values of μ.

We note finally that in view of the argument based on condition (11) and eqns (3), it is vitally important that the stropping system (like that of Figure 2) should be such that changes in Θ consequent on increase of F are zero or very small.

2.4 CLASSICAL DIVERGENCE

Divergence of the container in a combined $y-\psi$ mode will occur if F is such that

$$\left|\chi\,\underset{\sim}{E} + \mu\,\underset{\sim}{C}\right| \leqslant 0 \quad \ldots\ldots\ldots\ldots\ldots\ldots\ldots\ldots \quad (12)$$

On using eqns (4h) and (4i) and expanding the above determinant, we obtain the following condition for the absence of divergence:-

$$\frac{\mu}{\chi}\left[C_{22}(1+r) - (\alpha-\beta r)C_{12}\right] + \varepsilon^2\Sigma^2(1+r)^2 + r(a+b)^2 > 0 \quad \ldots\ldots \quad (12a)$$

If divergence is not to be possible, the term in the square bracket must be positive. For the 5:2:2 and 5:1:1 containers in nose-down attitudes, Θ, such that $C_{N\dot{\psi}}$ is negative, $C_{12} < 0$ while C_{22} may be positive or

negative - but about ten times smaller than $|C_{12}|$. Thus, principally, the requirement for no divergence will demand $\alpha-\beta r > 0$. However, condition (10a) requires $\alpha-\beta r < (1+r)R$ for the absence of undamped flutter. These requirements are clearly in conflict - the conflict being direct if $R = 0$ (i.e. G coincident with C). If flutter is to be ruled-out at the expense of the possibility of divergence, the divergence speed may be raised by increasing a+b and/or ε, the strop spacings.

From the above argument, a tentative divergence criterion is seen to be

$$r > \frac{a - \frac{h}{2}\tan(\theta-\Theta)}{b + \frac{h}{2}\tan(\theta-\Theta)} \qquad \ldots\ldots\ldots\ldots\ldots\ldots \quad (13)$$

2.5 A COMPUTER STUDY OF THE LATERAL FLUTTER AND DIVERGENCE OF THE 5:2:2 AND 5:1:1 CONTAINER SHAPES

Figure 3 presents the pertinent aerodynamic information for the 5:2:2 and 5:1:1 container shapes obtained from the wind tunnel results of Refs 1 and 3. Table I summarises the required coefficient and derivative information. It should, however, be borne in mind that the above results apply to ideal, low turbulence, wind tunnel conditions. At low values of Θ, C_M and $C_{N\dot{\psi}}$ are highly sensitive to free stream turbulence intensity[3] and may be changed in sign as this increases. They may also change sign at low Θ due to small, steady, yaw departures, such as might result from helicopter sideslip or from a modest crosswind. Hence, we have allowed variations in the aerodynamic coefficients and derivatives in order sensibly to accommodate such effects.

All calculations were performed on a HP 9830A desk top computer - the program being based on eqns (3) and (4) and on the Routh discriminant method.

2.5.1 The 5:2:2 Container

For this shape, a Froude number range $0 < F < 10$ was studied in increments $\Delta F = 0.5$. The typical container has dimensions 20' x 8' x 8', and so $F = 10 \equiv V \approx 254$ ft/sec. Sea level conditions were assumed with $\rho = 23.8 \times 10^{-4}$ slug/ft^3 in order to provide a basis for estimates of μ. The μ-range studied was in fact 0.002 to 0.02 representing a 'full' weight of just over 10 tons and an 'empty' weight of just over one ton. In the 'standard' case, G was positioned at C with $a = b = 0.4$ and $\varepsilon = 0.2$. The 'standard' dimensionless strop length was $\ell = 1$ and the 'standard' dimensionless radii of gyration of the container were taken as $k_\psi = 0.289$ and $k_\phi = 0.15$. Initially, Θ was set at 12°, the appropriate aerodynamic coefficients being those of Table Ia, row 2.

The computations for this 'standard' case showed that flutter would not occur as μ was varied from 0.002 to 0.02, ℓ from 0.5 to 4, k_ψ from 0.15 to 0.4 and a, b were given the values 0.5, 0.3; 0.3, 0.5; 0.3, 0.3 as well as the standard values 0.4, 0.4. The absence of flutter is ascribable almost wholly to the negative value of C_M. When this was increased to positive values, flutter ensued. Making x overtly negative (G well aft of C) could also produce flutter. However, divergence did occur in the standard case; at F = 7, 9.75 for μ = 0.02 and 0.01

respectively, but not for $\mu = 0.005$ and 0.002. Shortening the strops ($\ell = 0.5$) eliminated divergence, lengthening them lowered the divergence speeds. Reduction of a + b also lowered the divergence speeds, but variation of a and b with a + b constant had little effect on divergence. Criteria (11) and (13) were found to hold in all cases. At face value, therefore, it appears that the 5:2:2 container may be carried stably on short strops ($\ell = 0.5$) with a and b in excess of 0.3. However, we cannot be too complacent about this, since turbulence[3] and other effects mentioned previously may reverse the sign of C_M.

We now define a modified 'standard' case, based on conditions of 10% free stream turbulence intensity, in which $C_D = 1.1$, $C_L = 0.3$, $C_M = 0.05$, $C_{y\bar{\psi}} = 3$, $C_{N\bar{\psi}} = 0.25$ with the other coefficients as per Table Ia, row 2. Also, we view $\mu = 0.01$ as 'standard'. That this modified system is highly flutter-prone is amply evident from Figure 4. In the modified standard case, flutter occurs at $F = 5.2 \equiv F_F$; the undamped prediction being $F = 4.9 \equiv F_U$. At $F = 0.5$, 2, 3, 4.5 and 10, r was found to be 1.23, 1.17, 1.10, 0.96 and 0.48 respectively while the R.H.S.'s of criteria (11) and (13) were found to be 1.24, 1.18, 1.12, 1.01 and 0.57 respectively, so that the criteria rightly indicate flutter, but no divergence.

Figures (4a) and (4b) show that increases of μ and ℓ both lower the flutter speed, as might have been expected. Figure (4c) shows that G forward of C is highly stabilising and that G aft of C is destabilising - as in classical wing flutter. With $x = 0.1$, $z = 0$, flutter is eliminated, but it will re-appear if C_M and $C_{N\dot{\psi}}$ are overtly large of if $C_{y\bar{\psi}}$, $-C_{N\dot{\psi}}$ and $C_{y\dot{\psi}}$ are untypically small. In the case where $C_{N\dot{\psi}} = -0.01$ and $C_{y\dot{\psi}} = 0$, the flutter at $F = 7.25$ is of the damping/inertia coupled type and cannot be predicted by undamped theory and hence by criterion (11). That this flutter is weak is evident from the fact that F_F is raised to 8 when $C_{y\dot{\psi}} = 0.04$ and is eliminated completely when $C_{N\dot{\psi}} = -0.1$. The case where $x = -0.1$ is of particular interest since both flutter and divergence occur; flutter ($F_F = 3.4$) preceding divergence ($F_D = 7.5$). The comparison below shows the validity of criteria (11) and (13) in this case:-

F	1	3	3.4	4	5	7	7.5	9
R.H.S.(11)	2.08	1.89	1.80	1.75	1.60	1.31	1.24	1.06
r	2.07	1.80	1.70	1.61	1.42	1.07	0.99	0.79
R.H.S.(13)	1.22	1.12	1.08	1.04	0.96	0.79	0.75	0.65

Figure (4d) shows that increase of A + b (a = b) raises F_F, as expected, while Figure (4e) shows that if b/a is varied with a + b = 0.8 the effect is mildly destabilizing with respect to the standard case, $b/a = 1$, in which G (and C) is central between the strops. Figure (4f) shows, in comparison with Figure (4d) that increasing k_ψ with G at C is similar to the effect of decreasing a + b (a = b); i.e. it is destabilizing. Figure (4g) shows that increased yaw damping raises F_F, but that if $|C_{N\dot{\psi}}| < 0.15$ (approximately), damping/stiffness coupled flutter may occur; this not being predictable by undamped theory or criterion (11): For although criterion (11) appears to hold (i.e. undamped flutter exists), the phenomenon which it relates to is not the phenomenon which actually occurs. However, the flutter in this case is of the weak variety.

Figure (4h) shows the effect of C_M; increase being destabilising. If C_M is slightly negative, flutter persists, but at $C_M = -0.05$ flutter has been replaced by divergence at $F_D = 8.5$ as the basic mechanism of container instability. Further decrease of C_M lowers the divergence speed - physically by de-tensioning the windward strops. At $C_M = 0.1$, a numerical check showed that damping/stiffness flutter could occur if $|C_{N\dot{\psi}}|$ were sufficiently small - this not being predicted by criterion (11). Figures (4i) and (4j) show the C_D and C_L effects - these effects being respectively destabilising and stabilising, but very small. Figures (4k) and (4ℓ) show the $C_{y\overline{\psi}}$ and $C_{N\overline{\psi}}$ effects - both being destabilising, the latter much more so than the former. Since $C_{N\overline{\psi}}$ is greatly affected by turbulence or yaw angle effects, the importance of this derivative is considerable.

The above parameter variation study is by no means complete. We recognise, for example, that frequency ratio is a vital factor in all flutter phenomena, and we might therefore expect to see many of the effects 'turned around' if, at $F = 0$, the ψ-dominant mode has a natural frequency less than that of the y-dominant mode in the 'standard' case. In our 'standard' case, the ψ-frequency dominated the y-frequency at $F = 0$, and the stropping configuration might well be designated 'hard stropping'. For hard stropping, flutter occurs when, as F is raised the ψ-frequency is reduced to coalescence with the y-frequency. More importantly, we have shown that the serious flutter cases are predicted by undamped theory and hence have validated criterion (11) (and indeed, criterion (13)) which may now be applied generally.*

From a practical viewpoint, it appears that if it could be arranged that 5:2:2 container shapes be loaded such that G is displaced from C by $x = 0.1$, then stable carriage would be assured in the 'standard' configuration described above.

2.5.2 The 5:1:1 Container

When considering this shape, we bear in mind that the usual dimensions are 40' x 8' x 8' so that the possibility of 'hard stropping' is a remote one, bearing in mind the dimensions of the helicopter. Hence we attempt a 'soft stropping' solution of the stability problem: i.e. one in which, at $F = 0$, the y-frequency exceeds the ψ-frequency. However, $a + b$ cannot be too small for fear of divergence induced by sidewinds. Preliminary calculations showed that $a + b = 0.4$ might be suitable, but for reasons of illustrating the complexity of the 'soft-stropping' flutter phenomenon, we choose $a + b = 0.52$. For a 40' x 8' x 8' container, this implies a stropping distance $\overline{a} + \overline{b} = 20.8$ ft, which is not excessive. Again, for such a container, a Froude number $F = 10$ implies $V \approx 360$ ft/sec and so the F range of practical interest might be (0, 5) in this case.

As previously, we consider $\mu \in (0.002, 0.02)$ and take $k_\psi = 0.289$, but now $k_\phi = 0.07$. In the 'standard' case, G is positioned at C with $a = b = 0.26$ $\varepsilon = 0.1$, $\ell = 1$ and $\Theta = 7^\circ$ - the aerodynamics being defined in Table Ib, row 2. Computations showed that the standard case, thus defined was flutter and divergence free up to $F = 10$ and could not be made to exhibit instability

*Except, perhaps, in cases for which the ψ and y frequencies are very close together at $F = 0$. This is a well-known restriction on the use of undamped theory.

by varying μ, but could be made to diverge by increasing ℓ or reducing $a+b$ - moreso at the larger values of μ. Thus, at face value, it seems fortuitously that we have hit upon a configuration for stable conveyance of the container, as in the 5:2:2, but here again we have to contend with the vagaries of the aerodynamics due to turbulence and sidewind effects - notably of C_M and $C_{N\overline{\psi}}$. For this reason, we again adopt a modified standard case wherein $C_M = 0.02$, with all other aerodynamic coefficients and derivatives as given in Table Ib, row 2. That the modified standard case is flutter prone is evident from Figure 5. In fact, it flutters at $F = 6$, when the standard μ, i.e. 0.01, obtains.

Figures (5a), (5i) and (5k) show the μ, C_D, C_L and $C_{y\overline{\psi}}$ effects, respectively, and these, being of the same essential shapes as in the 5:2:2 case, require no further comment. Figure (5b) shows the small effect of increase of ℓ on F_F, but the 'nose' of the $F_F \sim \ell$ curve near $\ell = 4$ signifies a change to divergence for further increase of ℓ. Figure (5c) shows the effect of G position (longitudinal) - and this is a much more complex picture than that for 'hard-stropping' (Figure (4c)). A slight movement forward of G is very beneficial, but if $x > 0.9$, low-F flutter is encountered. Rearward movement has little effect for $x > -0.05$, but if $x < -0.05$, low-F divergence results. Undamped theory is conspicuously inaccurate in this case, although the essential branched nature of the flutter curves are reflected by it. Figure (5d) is likewise complex: as strop spacing is increased, F_F decreases rapidly. This is a consequence of soft-stropping, for as $a+b$ is increased, the ψ-frequency is raised towards coalescence with the y-frequency. This effect is precisely opposite to that in the hard-stropping case (Figure (4d)). Conversely, as $a+b$ is reduced, F_F is raised until, at $a = b \approx 0.08$, divergence occurs.

Figure (5e) shows that the effect of b/a, with $a+b$ held at 0.52, is precisely opposite to that shown in Figure (4e). Now the case $b/a = 1$ is the least satisfactory if the aim is to raise F_F. Figure (5f) shows the effect of k_ψ which, for k_ψ greater than the standard value, 0.289, is precisely opposite to that of Figure (4f). At $k \approx 0.26$, $F = 0$ frequency coalescence has occurred; hence $F_u = 0$. For $k < 0.26$, the stropping is effectively 'hard' and the trend is as in Figure (4f). The yaw damping effect (Figure (5g)) is less serious here than in the 5:2:2 case. $C_{N\dot{\psi}}$ may be of zero value and the 'standard' flutter speed only marginally affected.

Figure (5h) shows the C_M effect - and this is more the same as in Figure (4h). However, there is a large region between $C_M = -0.03$ and zero in which flutter and divergence cannot occur. This is why our initial standard case, with $C_M = -0.002$, proved to be so stable! Again, we have highlighted the importance of C_M as a parameter in the container stabilisation problem. However, since C_M is so dependent on turbulence levels and parasitic yaw effects, it cannot really be used to effect in stabilisation exercises. Finally, Figure (5ℓ) shows the $C_{N\overline{\psi}}$ effect which, for modest excursions from the standard value of 0.14, exhibits opposite trends to those of Figure (4ℓ). This is because decrease of $C_{N\overline{\psi}}$ raises the ψ-frequency towards coalescence with the y-frequency, thus lowering F_F. If $C_{N\overline{\psi}} > 0.3$, flutter gives way to divergence.

Criteria (11) and (13) were found to be valid in all cases studied - as is evident from Figure 5 which shows that every flutter condition is accompanied by undamped flutter.

We conclude that the 5:1:1 shape of 40 ft major side may be carried stably in the standard configuration for F < 5. For G slightly forward of C, the chances of instability are reduced, but if G is overtly forward of C, the container could become highly unstable at low F.

2.6 OTHER MULTIPLE-STROP ARRANGEMENTS

It has already been stressed that if containers of the above type are to be conveyed stably in straight and level flight, it is desirable that Θ should not change appreciably with V. This will usually require a frame, pre-angled at Θ, to be attached to the helicopter - although there is scope here for research on stropping geometries which maintain Θ without need of such a frame. Clearly, three strops would suffice instead of four in the arrangement shown in Figure 2, but the more usual arrangement is of the twin-strop variety with lifting bar, as in Figure (1b). A simple variant of this arrangement (with or without lifting bar) is shown in Figure (6a), the nose down Θ being provided by a single rigid tie attached to the forward lifting position on the helicopter. If the lifting bar is light (or completely absent), the y and ψ modes will be as shown in Figure (6b). In this case, unlike the arrangement of Figure 2, ϕ is kinematically uncoupled from ψ and the ϕ effect in the y mode will be small.* The bifilar arrangement is such that if the container is rigid and all strops inextensible, the ψ-frequency is inversely proportional to $\bar{\ell}^{\frac{1}{2}}$ while the y-frequency is inversely proportional to $\{\bar{\ell} + \bar{\ell}_1 + (\frac{h}{2} + \bar{z}) \cos\Theta\}^{\frac{1}{2}}$ - a situation which favours the 'hard stropping' solution described earlier. The previous theory will apply, albeit with minor changes in the matrices $\underset{\sim}{A}$, $\underset{\sim}{B}$, $\underset{\sim}{C}$ and $\underset{\sim}{E}$ and hence in criteria (11) and (13). In the previous notation, and with $\ell_1 = \bar{\ell}_1/\bar{d}$, criteria (11) and (13) are modified to

$$r < \frac{a + \ell_1 S - R\gamma}{b - \ell_1 S + R\gamma} \quad \text{(flutter)} \qquad \ldots\ldots\ldots\ldots\ldots\ldots \quad (14)$$

$$r > \frac{a + \ell_1 S}{b - \ell_1 S} \quad \text{(divergence)} \qquad \ldots\ldots\ldots\ldots\ldots\ldots \quad (15)$$

where
$$\gamma\left\{\ell + \ell_1 + \frac{h}{2} C\right\} = \ell + \left(\ell_1 - \frac{h}{2}\right)(1 - C) \qquad \ldots\ldots\ldots\ldots \quad (16)$$

$$S = \sin(\theta - \Theta) \quad \text{and} \quad C = \cos(\theta - \Theta) \qquad \ldots\ldots\ldots\ldots \quad (16A)$$

By making $\bar{\ell}$ progressively smaller, the ψ-frequency is raised more rapidly than the y-frequency, until, when $\bar{\ell} = 0$, the ψ-frequency is infinite; i.e. yaw motions have been eliminated. We then have a special, parallel, version of Sheldon's 'V-strop' which eradicates y-ψ flutter. (Sheldon's V-strop arrangement[5] is sketched in Figure (6c)). The totality of the yaw restraint depends on the rigidity of the container and the inextensibility of the strops. Because the degree of yaw constraint is high, the transmissibility of freight aerodynamic loads into the helicopter is large, and it becomes necessary to consider ab initio the complete helicopter-freight system in the dynamical analysis, which should also include strop flexibility and the nonlinear effects of strop slackening. Such an analysis has been attempted in Reference 6. That the

*y-ϕ coupling is negligible from an aerodynamic, but not from a structural, viewpoint.

Sheldon strops obviate flutter in the ideal case has been proved by wind tunnel testing[3]. However, for the carriage of long containers (e.g. 40' x 8' x 8'), a 'soft stropping' arrangement has been shown to be feasible, and this, with its low transmissibility of yawing moments into the helicopter, militates in favour of the use of the Y strop (Figure (6b)).

2.7 SUMMARY OF PART I

We have presented an analysis of lateral flutter of rectangular container loads based on an idealised strop arrangement and quasi-steady aerodynamic theory. The flutter and divergence characteristics have been shown to be of a complex nature, and yet are predictable by use of undamped theory in the vast majority of cases. This has led to the presentation of necessary conditions for flutter and divergence, based wholly on longitudinal characteristics at equilibrium at any flight speed. These criteria are thought to be potentially useful for assessment of the lateral stability of more general loads supported by parallel strops. However, a prerequisite of lateral stability is the choice of Θ, the rigging incidence, such that the y and ψ motions per se are stable - and this will not always be possible in respect of dynamic stability. For example, it would be imprudent to carry a jeep upside down, even if in this position $C_{N\dot{\psi}}$ is optimally negative!! This leads us appropriately into Part II of this paper which concerns the requirement for aerodynamic research on three dimensional bluff bodies such as may be conveyed beneath helicopters.

3. PART II AERODYNAMIC RESEARCH REQUIREMENTS IN THE FIELD OF HELICOPTER UNDERSLUNG LOAD DYNAMICS

3.1 INTRODUCTION

In the first part of the paper, we studied a particular type of dynamic instability of a particular type of underslung load, i.e. lateral flutter of a multi-stropped rectangular container. This phenomenon was characterised by low values of frequency at fairly high forward speeds, i.e. by low frequency parameter, thus justifying our use of quasi-steady aerodynamic derivatives. In general, however, loads of every conceivable shape may be carried - often on single strop or otherwise simple suspension systems. Such loads may exhibit many types of dynamic instability behaviour, e.g. translational and rotational 'galloping', conventional and stall flutter, divergence and sundry instabilities[3] associated with unsteady separated flows at high values of frequency parameter. All of these phenomena might prove to be envelope-limiting and restrict flight speeds unduly. It is to this general picture that this part of the paper is devoted, for, in the view of the authors, much fundamental aerodynamic research is called for.

3.2 TYPES OF TOWED SHAPES AND THE STATE OF AERODYNAMIC KNOWLEDGE

The shapes that might be towed beneath helicopters may be classified broadly as follows:-

1. BLUFF (a) Sharp edged) oblate or prolate, convex or re-entrant -
) including possibility of through-flow,
(b) Curved) symmetric or unsymmetric, regular or
) irregular.

2. STREAMLINED (a) Plate-like: high aspect ratio
low " "

(b) Axi-symmetric or near axi-symmetric; solid or tubular, long or short.

It is clear that a shape might be classified both streamlined and bluff, depending on how it is towed. e.g. A 2:1 flat plate would be streamlined with aspect ratio 2 or 0.5 depending on whether its major axis is cross-wind or 'along wind', with the plane of the plate near horizontal or near the vertical plane containing the flight velocity vector, but bluff if the plane of the plate were normal, or nearly normal to this vector. Common sense might dictate that a plate load would surely not be carried in the latter configuration, but the authors have been told of many cases where loads have been conveyed (or attempts made to convey them) in the most unusual configuration!

The streamlined shapes will probably have $C_L > C_D$. Some bluff shapes might generate substantial C_L's, but, by and large, $C_D > C_L$. Beyond these statements, classification proves naturally to be highly complex for reasons alluded to in the previous paragraph.

Streamlined shapes on the whole are amenable to the aerodynamic theories of aeronautics. Some of the plate-like shapes will admit a full aerodynamic solution - including frequency-parameter-dependent or indicial aerodynamics in classical form. Others might be amenable to lifting surface theories. The situation is not so clear cut, however, should the plate stall. The axi-symmetric streamlined shapes are sometimes amenable to slender-body aerodynamics solutions, including unsteady effects. Certain axi-symmetric, prolate bluff shapes may be tackled by using viscous crossflow theory[2], but only in respect of static aerodynamics - and even then the moments may be grossly inaccurate due to separation bubble effects which cannot be allowed for. Lifting line theory may be used in some cases to obtain some of the damping derivatives (e.g. thick plates, L_p; Sheldon) but only for small frequency parameters. For the most part, however, theoretical aerodynamics techniques will not be applicable and one must resort to experimental, wind tunnel methods.

On the experimental side, the U.S. sponsored contract work mentioned in Section 1 has perhaps provided the 'lions share' of available information - naturally oriented towards military-type cargo shapes. Such shapes are predominantly bluff: regular in the case of rectangular containers and irregular in the case of bulldozers, jeeps, howitzers and 'human' loads. Many of these bluff-irregular loads also have re-entrant characteristics which can give rise to stability problems stemming from re-attaching shear layers. However, the available information (References 1, 2, 7) is usually restricted to steady aerodynamics. Indeed, References 3 and 4 are the only known papers dealing with the unsteady aerodynamics of bluff loads - a very sorry state of affairs in view of the fact that the frequency-parameter dependence of the aerodynamic forces and moments was shown to be considerable in the case of rectangular containers.

So far as flutter is concerned, the first part of the paper shows that the steady information might suffice, provided frequency is low. However, rate derivatives are required, and the only papers which provide them are References 3, 4 and 6 - and only then for certain rectangular containers. Thus, even on this 'low frequency front', the situation is currently bleak. For higher frequency parameter regimes, it is even bleaker.

We appreciate that it would be impossible to cover all possible shapes under headings 1 and 2 above and thus, in the final section, we attempt to point to areas in which additional research is most urgently required.

3.3 AERODYNAMIC RESEARCH: PRESSING NEEDS

The needs for additional effort are summarised in the list below - not necessarily in the order of priority:

(i) Quasi-steady rate derivatives for cargo shapes typified by vehicles, armaments, etc., for which steady aerodynamic information is already available. (References 2, 8).

(ii) Novel, quasi-experimental, quasi-theoretical methods, based on steady aerodynamic information, for prediction of unsteady aerodynamic behaviour of bluff shapes of various types. (E.g. Ref. 3, Section 7 and Ref. 4) Such could obviate the need for extended unsteady aerodynamics measurements.

(iii) More information on the aerodynamics of curved bluff bodies, with emphasis on Reynolds number effects. (Reference 9)

(iv) Unsteady aerodynamics measurements for certain of the more common shapes.

(v) Model and flight tests on freely suspended shapes.

We should stress that the accepted practice of providing merely static aerodynamic information on particular shapes (e.g. Reference 1), while undoubtedly important, does need to be supplemented with rate derivative measurements.

Finally, in Part I of the paper, the importance of stropping configuration was highlighted. Much more effort could be deployed in the area of strop design. The Sheldon 'V strop' appears to offer a solution to many of the ills implied in Section 3.2, simply by dint of mechanical constraint. This work should surely be followed-up beyond Reference 6; this need being closely allied to a requirement for additional effort on active control solutions employing the helicopters ASE or extraneous devices such as 'active arms'.

4. CONCLUDING COMMENTS

We have addressed the problems of aerodynamic instability of helicopter underslung loads (i), via a in-depth study of lateral flutter of rectangular containers in Part I, and (ii), via a call for more

aerodynamic research in Part II. The salient feature of Part I is the emergence of strop tension criteria for flutter (and to a lesser extent for divergence) based on undamped theory: these criteria are thought to be new and potentially useful. The salient feature of Part II is our view of the current state of the art of the unsteady aerodynamics of bluff shapes and the need for more research effort.

It is hoped that this paper will act as a catalyst towards revitalisation of research in the entire area of underslung load dynamics with a view to replacing current ad hoc flight and wind tunnel test procedures by a more systematic approach.

5. REFERENCES

1. G.H. Laub and H.M. Kodani — 'Wind Tunnel Investigation of Aerodynamic Characteristics of Scale Models of Three Rectangular Shaped Cargo Containers' NASA TM X-62, 169; July 1972.

2. D.T. Liu — 'In-flight Stabilisation of Externally Slung Helicopter Loads' USAAMRDL Tech. Report 73-5, Contract DAJA02-70-C-0067; May 1973.

3. D. Chan, J.W. Flower and A. Simpson — 'Aerodynamically Induced Motions of Bluff Bodies Suspended Beneath Helicopters'. Final Tech. Report. USAA Contract No. DAJA37-73-C-0477; Oct. 1975.

4. A. Simpson and J.W. Flower — 'Unsteady Aerodynamics of Oscillating Containers and Application to the Problem of Dynamic Stability of Helicopter Underslung Loads' AGARD CP 235, Paper 13, 1978.

5. D.F. Sheldon, and J. Pryor — A Wind Tunnel Investigation of Yaw Instabilities of Box-shaped Loads Underslung from a Helicopter on a Tandem Suspension' RMCS Tech. Note AM/62, Dec. 1974, R.M.C.S., Shrivenham, U.K.

6. A. Prabhakar — 'A Study of the Effects of an Underslung Load on the Dynamic Stability of a Helicopter' Ph.D. Thesis, R.M.C.S., Shrivenham, U.K. June 1976.

7. D.F. Sheldon — 'A Study of the Stability of a Plate-like Load Towed Beneath a Helicopter' Ph.D. Thesis, University of Bristol, June 1968.

8. G.H. Laub and H.M. Kodani — Wind Tunnel Investigation of Aerodynamic Characteristics of a Scale Model of a D5 Bulldozer and an M109 Self-propelled 155 mm Howitzer' NASA TMX-62, 330; Jan. 1974.

9. P.W. Churms and R.K. Harris — 'An Investigation into the Flow Around Axi-symmetric Bluff Bodies' Report No. 223, 1978, Department of Aeronautical Engineering, University of Bristol, U.K.

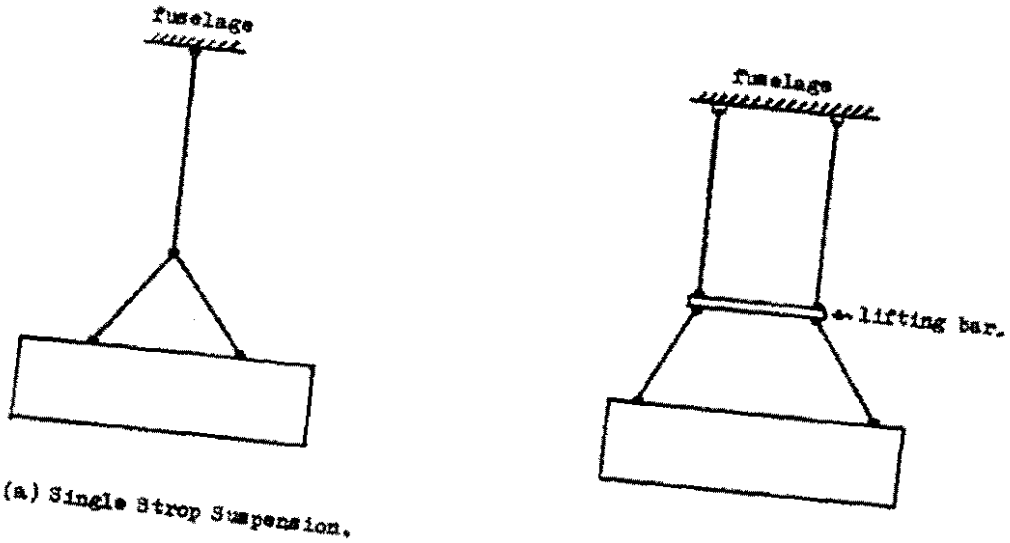

(a) Single Strop Suspension.

(b) Twin Strop Suspension.

FIGURE 1.

SINGLE AND TWIN STROP SUSPENSIONS.

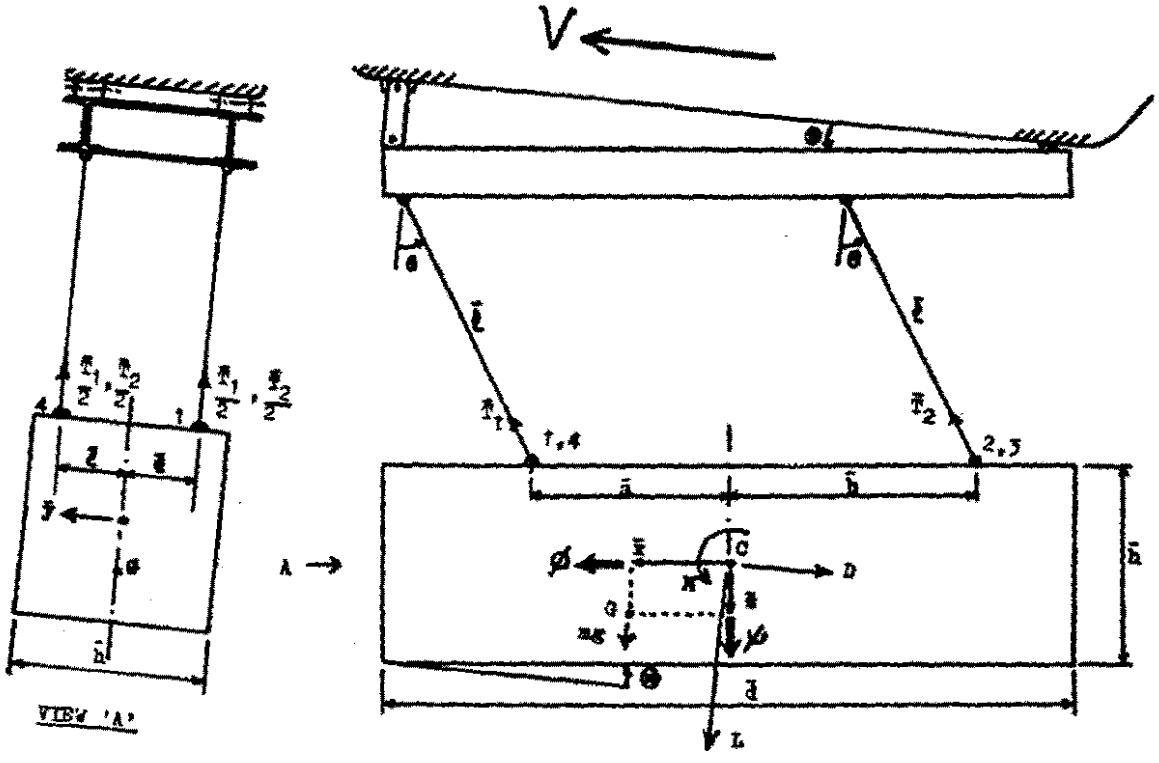

FIGURE 2

IDEALISED FOUR-STROP (PARALLEL) SYSTEM.

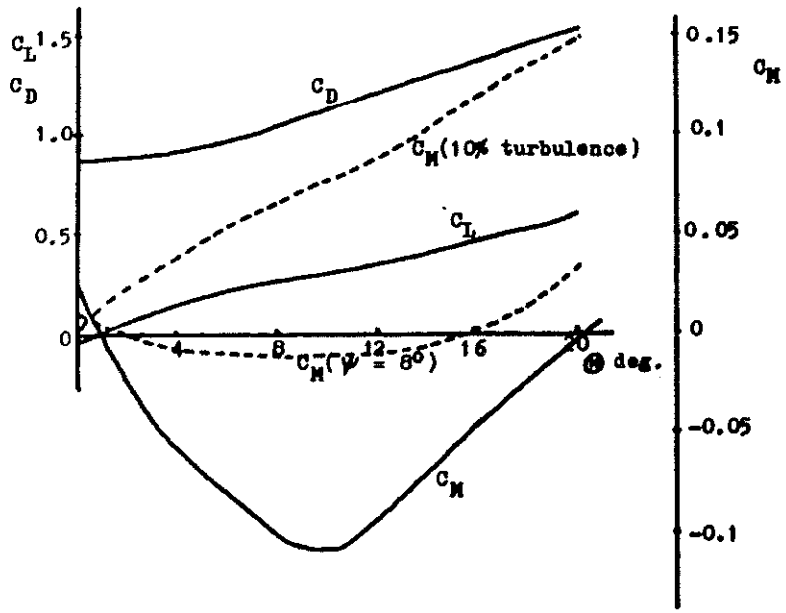

(a) Lift, Drag and Pitching Moment Coefficients For 5:2:2 Container at Zero Yaw Angle.

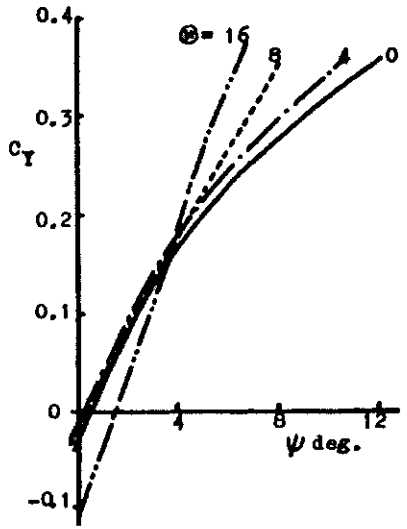

(b) Sideforce Coefficient for 5:2:2 Container

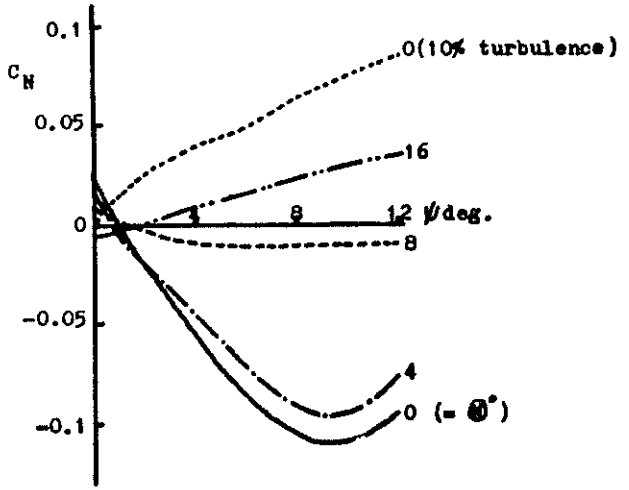

(c) Yawing Moment Coefficient for 5:2:2 Container

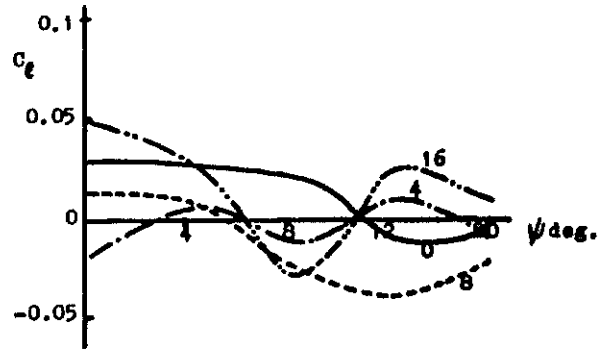

(d) Rolling Moment Coefficient for 5:2:2 Container.

FIGURE 3.

AERODYNAMIC CHARACTERISTICS OF 5:2:2 AND 5:1:1 CONTAINER SHAPES (AFTER LAUB AND KODANI [1]).

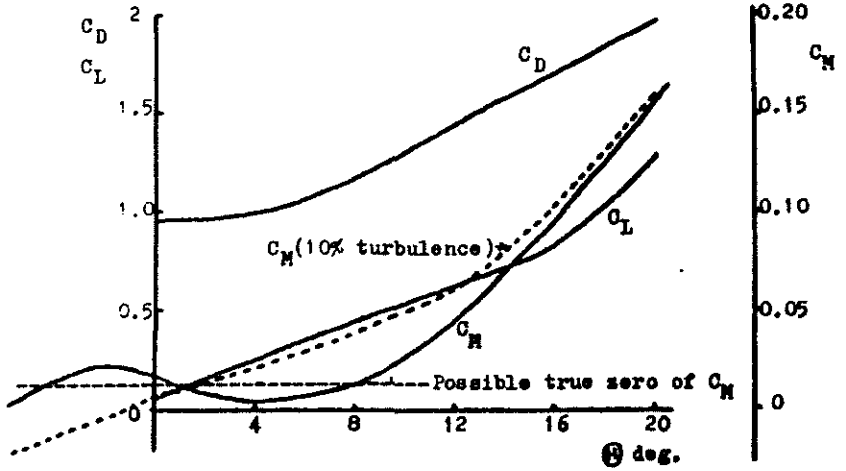

(e) Lift, Drag and Pitching Moment for 5:1:1 Container at Zero Yaw.

FIGURE 3

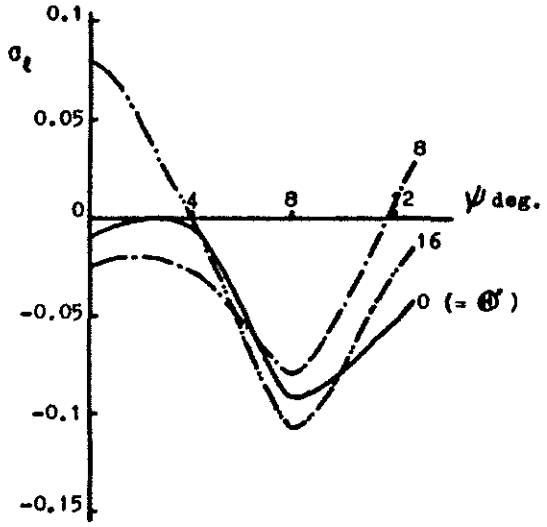

(h) Rolling Moment Coefficient for 5:1:1 Container.

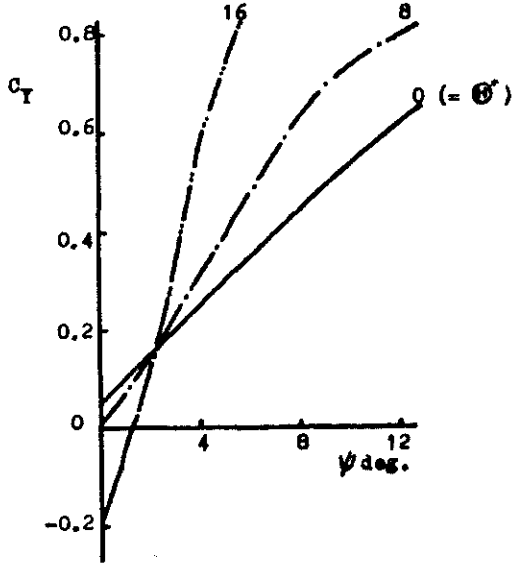

(f) Sideforce Coefficient for 5:1:1 Container.

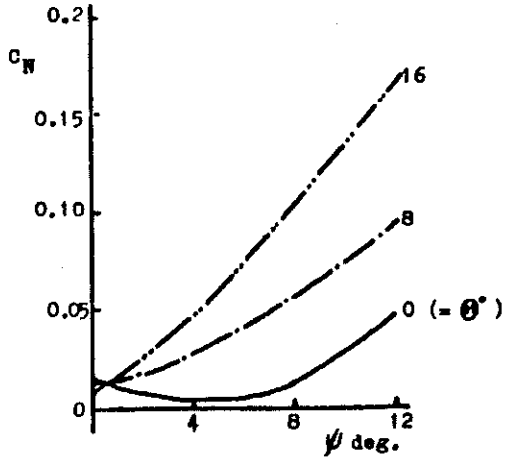

(g) Yawing Moment Coefficient for 5:1:1 Container.

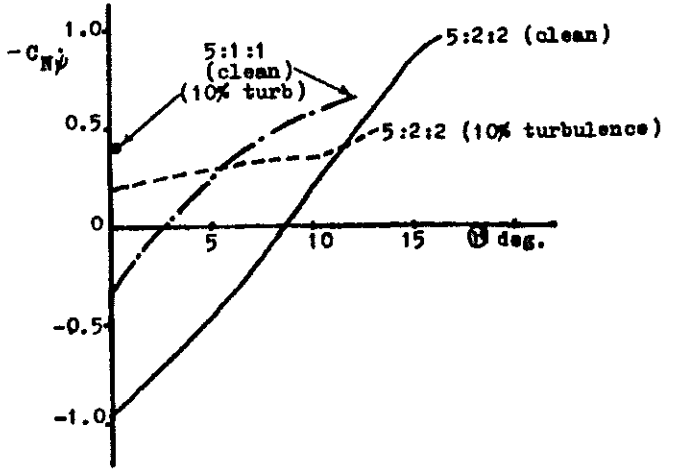

(i) Yaw Damping Coefficients for 5:2:2 and 5:1:1 Containers in Clean and Turbulent Flows. (Smoothed Results from Reference 3).

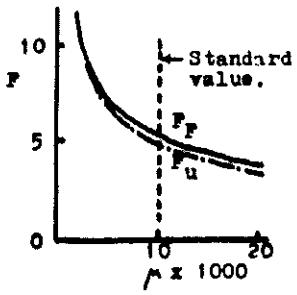

(a) μ Effect.

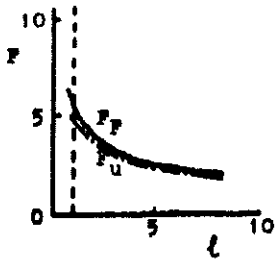

(b) ℓ Effect.

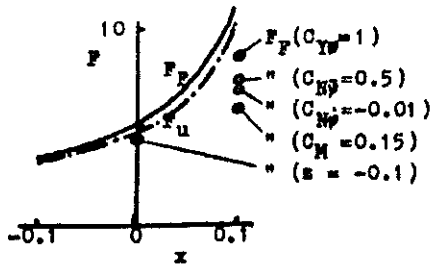

(c) G Position (x) Effect.

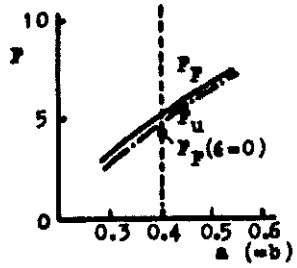

(d) Strop Spacing (a+b) Effect.

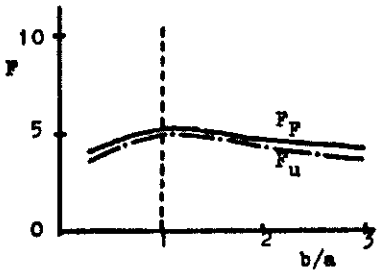

(e) Strop Position Effect (a+b = 0.8)

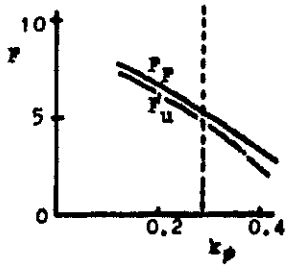

(f) Moment of Inertia Effect With G at C.

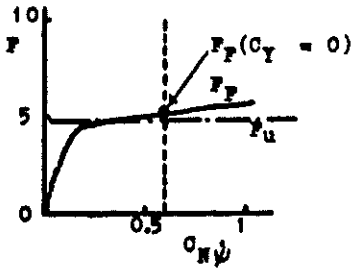

(g) Yaw Damping Effect.

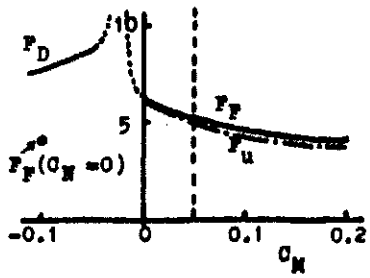

(h) C_N Effect.

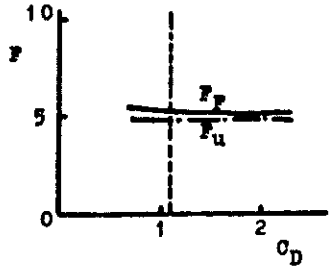

(i) C_D Effect.

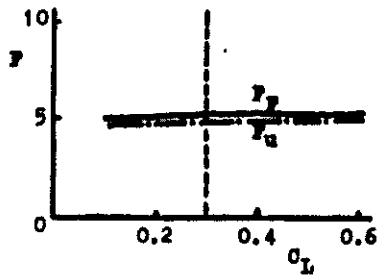

(j) C_L Effect.

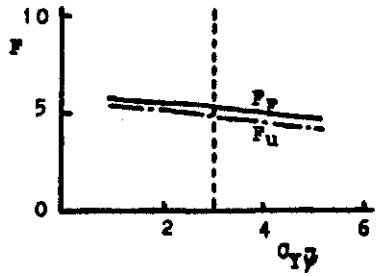

(k) $C_{Y\dot{\beta}}$ Effect.

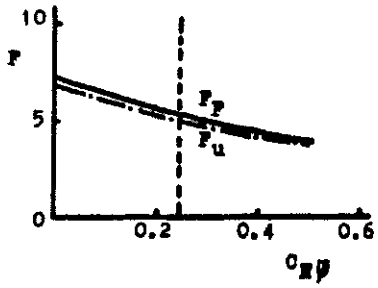

(l) $C_{N\dot{\beta}}$ Effect.

FIGURE 4

VARIATIONS OF STABILITY CHARACTERISTICS OF 5:2:2 CONTAINER AS IMPORTANT PARAMETERS ARE VARIED ABOUT THE 'STANDARD' CONFIGURATION.

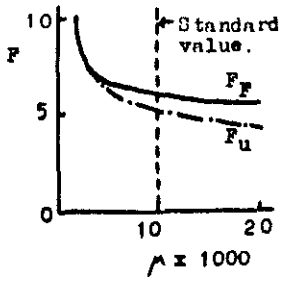

(a) μ Effect.

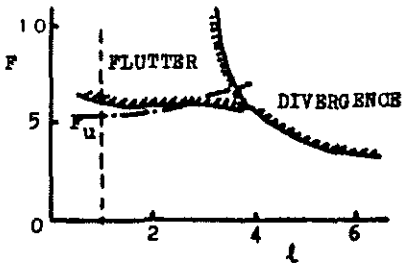

(b) ℓ Effect.

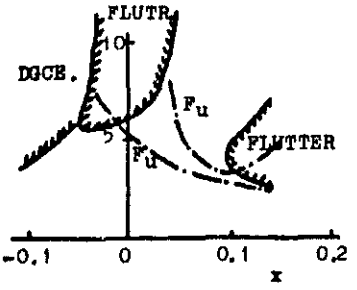

(c) G Position (x) Effect.

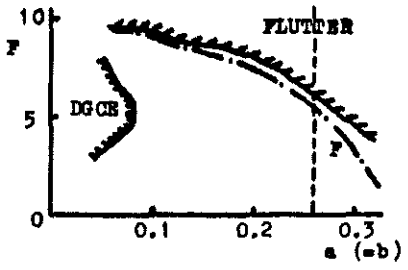

(d) Strop Spacing (a+b) Effect.

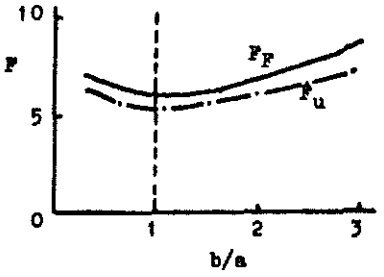

(e) Strop Position Effect (a+b = 0.52).

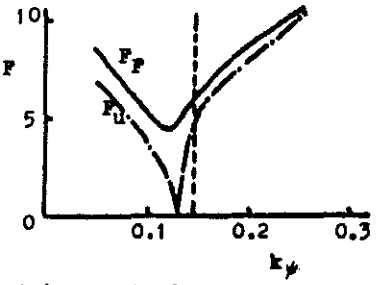

(f) Moment of Inertia Effect With G at C.

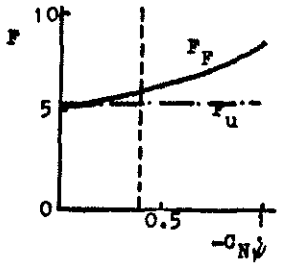

(g) Yaw Damping Effect.

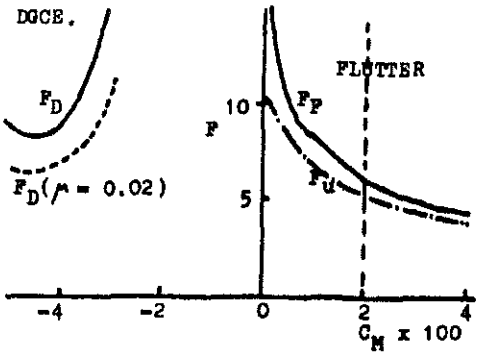

(h) C_M Effect.

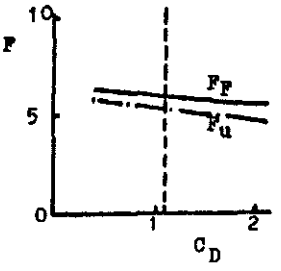

(i) C_D Effect.

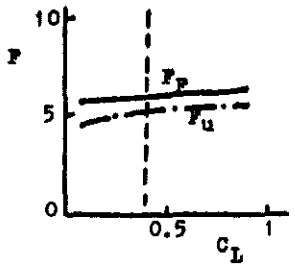

(j) C_L Effect.

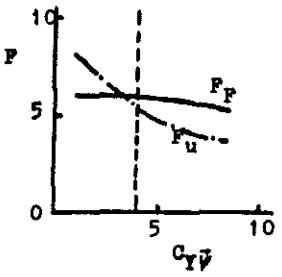

(k) $C_{Y\dot{\psi}}$ Effect.

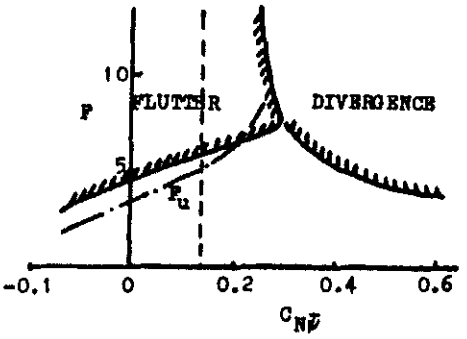

(l) $C_{N\dot{\psi}}$ Effect.

FIGURE 5

VARIATIONS OF STABILITY CHARACTERISTICS OF 5:1:1 CONTAINER AS IMPORTANT PARAMETERS ARE VARIED ABOUT THE 'STANDARD' CONFIGURATION.

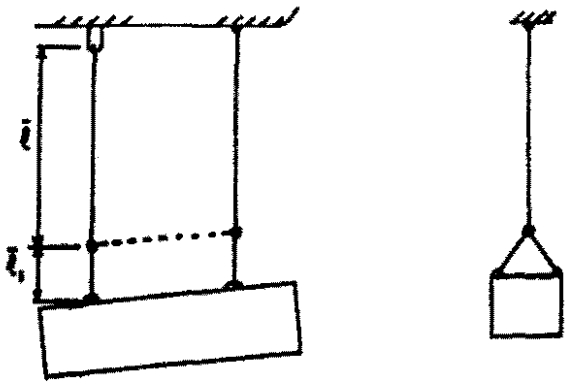

(a) Parallel Twin Strop.

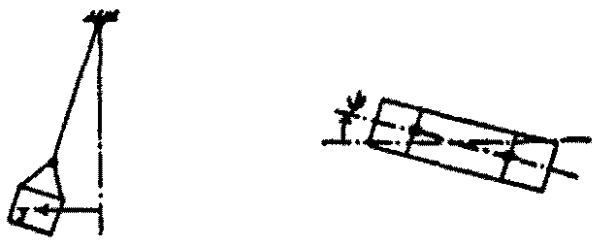

(b) Oscillation Modes (Lateral) of Parallel Twin Strop System Without Lifting Bar.

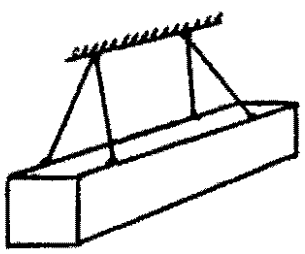

(c) Sheldon's V - Strop.

FIGURE 6

SOME POSSIBLE STROP CONFIGURATIONS.

TABLE I COEFFICIENT AND DERIVATIVE ESTIMATES FOR RECTANGULAR CONTAINERS

(a) 5 : 2 : 2 CONTAINER AT $\psi = 0$

Θ°	C_D	C_L	C_M	$C_{\bar{y}\bar{\psi}}$	$C_{\bar{N}\bar{\psi}}$	$C_{\bar{\ell}\bar{\psi}}$	$C_{N\dot{\psi}}$	$C_{y\dot{\psi}}^*$
10	1.125	0.3	- 0.109	2.72	- 0.287	0	- 0.2	0.3
12	1.2	0.35	- 0.093	3.4	0.05	- 0.14	- 0.6	1.2
16	1.37	0.45	- 0.046	4.15	0.22	- 0.287	- 0.8	1.5

(b) 5 : 1 : 1 CONTAINER AT $\psi = 0$

Θ°	C_D	C_L	C_M	$C_{\bar{y}\bar{\psi}}$	$C_{\bar{N}\bar{\psi}}$	$C_{\bar{\ell}\bar{\psi}}$	$C_{N\dot{\psi}}$	$C_{y\dot{\psi}}^*$
5	1.02	0.3	- 0.005	3.3	- 0.08	0.2	- 0.2	0.3
7	1.10	0.4	- 0.002	4.01	0.143	0.14	- 0.4	0.8
9	1.23	0.5	+ 0.01	5.2	0.210	0.05	- 0.5	1.0